

## Supplementary Online Content

Herberg JA, Kaforou M, Wright VJ, et al; IRIS Consortium. Diagnostic accuracy of a 2-transcript host RNA signature for discriminating bacterial vs viral infection in febrile children. *JAMA*. doi: 10.1001/jama.2016.11236.

**eAppendix.** Members of the Study Consortium

**eMethods**

**eStatistical Methods**

**eFigure 1.** Principal Components Analysis of the Samples in the Discovery Set

**eFigure 2.** Heatmaps Showing Clustering of the Training and Test Datasets Based on the Bacterial vs. Viral 38-Transcript Signature

**eFigure 3.** Elastic Net Prediction Value and Receiver Operator Characteristic Curves Based on the 38-Transcript Signature Applied to the Definite Bacterial and Viral Groups

**eFigure 4.** Disease Risk Scores and Receiver Operator Characteristic Curves Based on the 2-Transcript Signature Applied to Training Set

**eFigure 5.** STARD Flow Diagrams and Assessment of Diagnostic Test Accuracy

**eFigure 6.** Principal Component Analysis of Meningococcal and IRIS Validation Samples After Merging With Combat

**eFigure 7.** Disease Risk Scores and Receiver Operator Characteristic Curves Based on the 2-Transcript Signature Applied to Children With Gram-Negative And Gram-Positive Infection

**eFigure 8.** Disease Risk Scores and Receiver Operator Characteristic Curves Based on the 2-Transcript Signature Applied to Additional Validation Datasets

**eFigure 9.** Performance of the Disease Risk Score in Relation to Severity of Illness in the IRIS Validation Set

**eFigure 10.** Performance of the Disease Risk Score in Relation to Day of Illness in the IRIS Validation Set

**eTable 1.** Demographic and Clinical Features of the Validation Groups

**eTable 2.** Viral and Bacterial Causative Pathogens in Patients in the Definite Bacterial and Viral Groups in the Discovery and IRIS Validation Cohorts

**eTable 3.** 38-Transcript Signature for Distinguishing Bacterial From Viral Infection

**eTable 4.** Diagnostic Performance of the Bacterial vs. Viral 38-Transcript Elastic Net and Disease Risk Score 2-Transcript Signatures in the Training, Test and IRIS Validation Datasets

**eTable 5.** Gene Ontology (GO) Biological Process Terms Analysis

**eTable 6.** Additional Validation and External Microarray Datasets

**eTable 7.** Performance of Clinical Features in Relation to Disease Risk Score in Patients With Indeterminate Infection Status (Combined Probable Bacterial, Unknown, and Probable Viral Groups)

**eReferences**

This supplementary material has been provided by the authors to give readers additional information about their work.

## **eAppendix. Members of the Study Consortium**

### **IRIS Consortium members**

**Imperial College London (UK)** Michael J Carter, Lachlan JM Coin, Hariklia Eleftherohorinou, Erin Fitzgerald, Stuart Gormley, Jethro A Herberg, Martin L Hibberd, Clive Hoggart, David Inwald, Victoria A Janes, Kelsey DJ Jones, Myrsini Kaforou, Sobia Mustafa, Simon Nadel, Stéphane Paulus, Nazima Pathan, Joanna Reid, Hannah Shailes, Victoria J Wright, Michael Levin.

**Southampton (UK)** Saul Faust, Jenni McCorkill, Sanjay Patel.

**Oxford (UK)** Andrew J Pollard, Louise Willis, Zoe Young.

**Micropathology Ltd (UK)** Colin Fink, Ed Sumner.

**University of California San Diego (UCSD) and Rady Children's Hospital, La Jolla, California (USA)**

John T. Kanegaye, Chisato Shimizu, Adriana Tremoulet, Jane Burns.

**Hospital Clínico Universitario de Santiago (Spain)** Miriam Cebey Lopez, Antonio Salas, Antonio Justicia Grande, Irene Rivero, Alberto Gómez Carballa, Jacobo Pardo Seco, José María Martín Sánchez, Lorenzo Redondo Collazo, Carmen Rodríguez-Tenreiro, Lucia Vilanova Trillo, Federico Martín Torres.

**Academic Medical Centre (AMC) Amsterdam (Netherlands)** Anouk M Barendregt, Merlijn van den Berg, Taco Kuijpers and Dieneke Schonenberg.

**London School of Hygiene and Tropical Medicine, London (UK)** Martin L Hibberd.

**Newcastle upon Tyne Foundation Trust Hospitals and Newcastle University, Newcastle upon Tyne (UK)** Marieke Emonts.

### **Linked to IRIS consortium as GENDRES consortium member**

Enrique Bernaola Iturbe, Laura Moreno Galarraga, Jorge Álvarez (Hospital Materno Infantil Virgen del Camino, Pamplona); Teresa González López, Delfina Suarez Vázquez, Ángela Vázquez Vázquez, Susana Rey García (Complejo Hospitalario Universitario de Orense), Francisco Giménez Sánchez, Miguel Sánchez Forte (Hospital Torrecárdenas, Almería); Cristina Calvo Rey, María Luz García García (Hospital Severo Ochoa de Madrid); Ignacio Oulego Erroz, David Naranjo Vivas, Santiago Lapeña, Paula Alonso Quintela, Jorge Martínez Sáenz de Jubera, Estibaliz Garrido García (Hospital de León); Cristina Calvo Monge, Eider Oñate Vergara (Hospital de Donostia, San Sebastián); Jesús de la Cruz Moreno, M<sup>a</sup> Carmen Martínez Padilla, Eugenia Villanueva Martínez, Ana González Espín (Complejo Hospitalario de Jaén); Manuel Baca Cots (Hospital Quirón, Málaga), David Moreno Pérez, Ana Córdón Martínez, Antonio Urda Cardona, José Miguel Ramos Fernández, Esmeralda Núñez Cuadros (Hospital Carlos Haya, Málaga); Susana Beatriz Reyes, María Cruz León León (Hospital Virgen de la Arrixaca, Murcia).

## eMethods

### Patient recruitment

#### *IRIS Discovery and IRIS Validation groups*

Children were classified as Definite Bacterial if they had a clinical syndrome consistent with SBI (sepsis with shock or severe focal infection), and if pathogenic bacteria were detected at a usually sterile site (such as blood or CSF, excluding surface swabs, endotracheal secretions, or broncho-alveolar lavage samples); patients without sterile-site bacteria but with the other features listed above were categorized as Probable Bacterial. Children were classified as Definite Viral if they had a viral clinical syndrome, displayed no bacterial features, and matching virus was identified; patients without detected viruses but with clinical features of viral infection were classified as Probable Viral. In the absence of sterile site bacteria, children with inconclusive clinical features were classified as Unknown Bacterial or Viral. We used a C-Reactive Protein (CRP) cut-off of above 60 mg/L for inclusion into the Probable Bacterial group, or exclusion from the Probable and Definite Viral groups; otherwise patients were categorized as Unknown. Inclusion in the Definite Bacterial group was irrespective of CRP. The indeterminate infection patients not selected for array were those with the most missing clinical data (Fig. 1B).

#### *Healthy controls*

In order to compare expression of identified biomarker genes with the healthy state and understand the direction of expression (up- or down-regulation), healthy children without intercurrent infection or recent immunization were recruited from the outpatient phlebotomy department (n=52). Data from healthy controls were not utilized in identification or validation of RNA expression signatures.

#### *Meningococcal Validation cohort*

We validated our expression signatures on children with meningococcal (gram-negative) infection (n=24), recruited to an earlier study at St Mary's Hospital, London, UK [1]. Following informed parental consent, and with approval of the hospital Local Research Ethics Committee (EC3263), venous blood was collected on admission and within 24 hours of onset of symptoms, from patients admitted to Pediatric Intensive Care Unit (PICU) at St Mary's hospital between December 2002 and May 2005 with suspected meningococcal sepsis, meningococcal meningitis or both. Group B meningococcus was detected in blood or CSF by culture or by bacterial DNA PCR amplification. Controls (used only for removal of array data batch effects) were healthy white adults recruited following informed consent [11 males, 10 females age median (IQR) 35.6 (30.8-44.5)].

#### *Inflammatory Validation cohort*

In order to establish if gene expression signatures could also distinguish children with bacterial infection from childhood inflammatory or vasculitic diseases, we used data from children with inflammatory diseases (eTable 1). Patients were recruited at pediatric centers in the Netherlands and USA under approvals by the Research Ethics Committees of UCSD (Human Research Protection Program #140220), Amsterdam (NL41846.018.12 and NL34230.018.10). The inflammatory syndromes in the cohort were a) Henoch Schönlein Purpura (HSP) that was diagnosed in children presenting with palpable purpura, typically over the buttocks and extensor surfaces in association with abdominal pain, arthralgia or renal abnormalities (hematuria and proteinuria); and b) Juvenile Idiopathic arthritis (JIA) that was defined according to International League of Associations for Rheumatology [2]. Patients for the JIA cohort were recruited at initial presentation with early arthritis. They were not treated with disease-modifying anti-rheumatic drugs, corticosteroids or biologicals. Some patients used simple non-steroidal anti-inflammatory drugs.

### RNA sample extraction and processing

Whole blood (2.5ml) was collected into PAXgene blood RNA tubes (PreAnalytiX, Germany), incubated for two hours, frozen at -20°C within six hours of collection, before storage at -80°C. Total RNA was extracted using PAXgene blood RNA kits (PreAnalytiX, Germany) according to the manufacturer's instructions. The

integrity and yield of the total RNA was assessed using an Agilent 2100 Bioanalyser and a NanoDrop 1000 spectrophotometer. After quantification and quality control, biotin-labeled cRNA was prepared using Illumina TotalPrep RNA Amplification kits (Applied Biosystems) from 500ng RNA. Labeled cRNA was hybridized overnight to Human HT12-V4 Expression BeadChip arrays (Illumina) [Discovery cohort, Inflammatory Validation cohort] or Human HT12-V3 Expression BeadChip arrays (Illumina) [IRIS validation cohort] or Human Ref-8 V3 Beadchip (Meningococcal validation cohort). After washing, blocking, and staining, the arrays were scanned using an Illumina BeadArray Reader according to the manufacturer's instructions. Using Genome Studio software, the microarray images were inspected for artifacts and QC parameters were assessed. No arrays were excluded at this stage.

## eStatistical Methods

### *Microarray pre-processing*

Data was analyzed using 'R' *Language and Environment for Statistical Computing (R) 3.1.2* [3]. Expression values were transformed to a logarithmic scale (base 2). Mean raw intensity values for each probe were corrected for local background intensities and robust spline normalization [4] (combining quantile normalization and spline interpolation) was applied. Principal Component Analysis (PCA) was used as part of the quality control process. PCA is an approach that allowed us to summarize our data and reduce the dimensionality (240 arrays x 48,000 probes, down to 240 arrays x no of principal components) in order to explore variance in the expression level [5]. Transcript expression profiles of all samples in the discovery dataset clustered together on PCA; regardless of the diagnostic group (eFigure 1). The arrays in the discovery dataset that correspond to patients with definite diagnosis were divided into 80%-20% for the identification and validation of expression signatures, resulting in a balanced training set ( $n_{\text{adenovirus}}=18$ ,  $n_{\text{flu}}=18$ ,  $n_{\text{RSV}}=22$ ,  $n_{\text{other viral}}=15$ ,  $n_{\text{bacterial gram-negative}}=20$ ,  $n_{\text{bacterial gram-positive}}=22$ ) and test set ( $n_{\text{adenovirus}}=5$ ,  $n_{\text{flu}}=5$ ,  $n_{\text{RSV}}=5$ ,  $n_{\text{other viral}}=4$ ,  $n_{\text{bacterial gram-negative}}=5$ ,  $n_{\text{bacterial gram-positive}}=5$ ).

### *Identification of expression signatures*

For the discovery dataset, we used transcripts that were measured on both V3 and V4 Illumina BeadChips (the intersection array IDs). Using the training set, we identified the transcripts that were differentially expressed between the definite viral and bacterial groups with  $|\log_2 \text{FC}| > 1$  and adjusted P-value  $< 0.05$ , using a linear model for expression, conditional on recruitment site. These thresholds were chosen to ensure that differential expression for selected variables could be distinguished using the resolution of other validation techniques (i.e. qPCR). The transcripts that fulfilled the above criteria were taken forward to variable selection with elastic net, using glmnet [6] package in R. The parameters of elastic net, which control the size of the selected model, were optimized via ten-fold cross-validation (CV). In order to identify a smaller signature, we applied an in-house forward selection algorithm to discover a transcript signature, Forward Selection – Partial Least Squares (FS-PLS) which was then implemented as a Disease Risk Score (DRS) – see below. In order to discover gene expression signatures using FS-PLS, the first iteration of the algorithm considers the expression levels of all transcripts (N) and initially fits N univariate regression models. The regression coefficient for each model is estimated using the Maximum Likelihood Estimation (MLE) function, and the goodness of fit is assessed by means of a t-test. The variable with the highest MLE and smallest p-value is selected first (SV1). Before selecting which of the N-1 remaining variables to use next, the algorithm projects the variation explained by SV1 using Singular Value Decomposition. The algorithm iteratively fits up to N-1 models, at each step projecting the variation corresponding to the already selected variables, and selecting new variables based on the residual variation. This process terminates when the MLE p-value exceeds a pre-defined threshold. The final model includes regression coefficients for all selected variables.

### *Disease Risk Score*

The DRS is based on subtracting the summed intensities of the down-regulated transcripts from the summed intensities of the up-regulated transcripts in the signature [7]. The disease risk score for individual *i* is:

$$\text{Disease Risk Score}^i = \sum_{k=0}^n \text{expr. value}_k^i - \sum_{l=0}^m \text{expr. value}_l^i \quad (1)$$

where:

**n** the number of up-regulated probes in the signature in disease of interest (bacterial infection) compared to comparator group (viral infection) and

**m** the number of down-regulated probes in the signature in disease of interest (bacterial infection) compared to comparator group (viral infection).

For the 2-transcript signature, the DRS was calculated by subtracting the log<sub>2</sub> transformed expression value of *IFI44L* from the log<sub>2</sub> transformed *FAM89A* expression value for every patient. The range of DRS in the population can be between: [the minimum *FAM89A* value – the maximum *IFI44L*, the maximum *FAM89A* value –the minimum *IFI44L* value]. Higher scores indicate bacterial assignment, whilst lower scores indicate viral assignment, with viral or bacterial assignment for a particular patient defined relative to the threshold value calculated in the reference group.

The performance of both the signatures was assessed on the 20% test and the IRIS validation dataset. The probable viral and bacterial groups as well as the unknown bacterial or viral infection group from the discovery cohort were assessed with the 20% test dataset. The thresholds for the classification throughout were calculated using the pROC package in R [8], employing the Youden's J statistic [9]. The optimal threshold was determined by the point in the ROC curve that maximizes the distance to the identity line (maximum of (sensitivities + specificities)). In the boxplots, boxes show median with 25th and 75th quartiles and whiskers show “range” (defined by ‘*boxplot*’ function in R). With a “range” value set at 1, the whiskers extend no more than 1 times the interquartile range.

The calculation of the confidence intervals for the sensitivity and the specificity was based on a stratified bootstrap resampling. For small sample sizes and perfect classification metrics, the bootstrapping method overestimates the lower bound of the confidence intervals (CIs), resulting to CIs from 100 to 100. For these cases (listed here), we used the exact binomial method for the calculation of the CIs: the specificity of the 2-transcript signature in the test set and its sensitivity in the validation set; the sensitivity of the 2-transcript signature in the GSE6269 and GSE40396 sets and the sensitivity of the 38-transcript elastic net signature in the test and validation sets.

#### *Analysis of IRIS validation dataset*

The IRIS validation dataset (analyzed using HT-12-V3 Illumina BeadChip arrays) was pre-processed and analyzed separately to the discovery dataset, using the same approach.

#### *Analysis of additional validation datasets*

To assess the performance of the signature in gram-negative bacterial infection, the IRIS validation dataset was merged with a dataset containing pediatric meningococcal infection and healthy controls. As the meningococcal and IRIS validation cohorts had been run on different versions of the Illumina chip, the data were merged for analysis using the ComBat method [10] to remove unwanted batch effects using transcripts common to the 2 platforms. The healthy controls in the IRIS validation set (Illumina HT12-V3), and the healthy controls in the meningococcal validation set (Illumina Ref-8) were used for the adjustment. One binary covariate was passed to ComBat which assigned samples to two groups - healthy, and disease (eFigure 6).

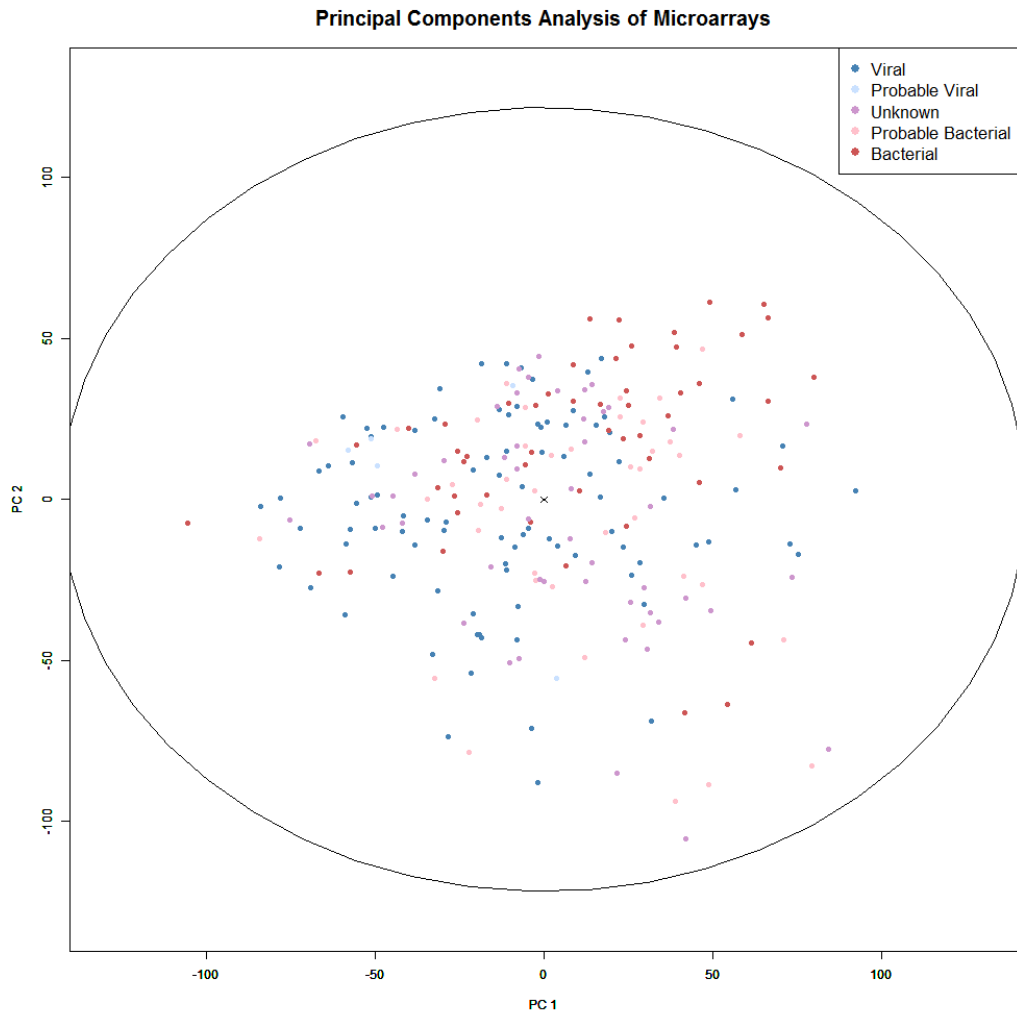
The inflammatory validation dataset contained JIA and HSP patients run on Illumina HT12-V4 arrays. These arrays were processed and normalized alongside the Discovery arrays, and the discriminatory power of the 2-transcript signature was applied without further pre-processing of array data.

To further validate the performance of the disease risk score based on the 2-transcript signature, we used publicly available microarray expression datasets with bacterial infections and comparator groups run simultaneously on the same platform to avoid the introduction of batch effects, as follows:

1. GPL570 [HG-U133\_Plus\_2] Affymetrix Human Genome U133 Plus 2.0 [11] (accession series GSE6269) dataset. The dataset consists of 22 pediatric cases, 10 viral and 12 bacterial; 7 children were diagnosed with Influenza A, 3 with Influenza B, 6 with *S. pneumoniae* and 6 with *S. aureus* infection. Gene identities for the two genes in our signature from the Illumina arrays were mapped to the Affymetrix dataset and “204439\_at” for *IFI44L* and “226448\_at” for *FAM89A* transcript ids were used. Despite differences in experimental design - the GSE6269 gene expression dataset was acquired from peripheral blood mononuclear cells using a non-Illumina platform, the 2-transcript signature DRS had a sensitivity of 100% (95% Confidence Interval (CI), 73.5 to 100) and a specificity of 90% (95% CI, 70 to 100), misclassifying only one viral patient with Influenza A (patient id: GSM173316). The Area Under the Curve (AUC) was 96% (95% CI, 85 to 100) (eFigure 7).
2. GSE40396 dataset. This includes 30 febrile children with viral infection (8 with adenovirus, 6 with enterovirus and 8 with HHV6) and 8 with bacterial infection (MRSA, MSSA, salmonella and *E.coli*) [12]. As the arrays used were Illumina HT12-V4, the same probe ids for *IFI44L* and *FAM89A* were identified. The 2-transcript signature had a sensitivity of 100% (95% CI, 63.1 to 100) and a specificity of 77.3% (95% CI, 59.1 to 95.5) and an AUC of 89.2% (95% CI, 75.6 to 98.3).
3. GSE22098 dataset. This includes 48 children (aged <17 years) with bacterial infection (*S. pneumoniae* and *S. aureus*) and 31 children with systemic lupus erythematosus [13], run on Illumina Beadchip HT12-V3 arrays. The same probe IDs for the two-transcript signature were available on both HT12-V3 and V4 arrays, and were applied to the data. The 2-transcript signature had a sensitivity for detection of bacterial infection of 93.5% (95% CI, 83.9 to 100) and a specificity of 96.1% (95% CI, 96.9 to 100) and an AUC of 96.6% (95% CI, 91.9 to 100).
4. GSE22098 dataset. This dataset includes patients with bacterial lower respiratory tract infection (LRTI) n=22 and viral LRTI n=71 run on Illumina Beadchip HT12-V4 arrays. As the arrays used were Illumina HT12-V4, the same probe ids for *IFI44L* and *FAM89A* were identified. The 2-transcript signature had a sensitivity for detection of bacterial infection of 90.1 (95% CI, 77.3 to 100) and a specificity of 80.3 (95% CI, 70.4 to 88.7) and an AUC of 89.8 (95% CI, 83.4-95.5).

**eFigure 1. Principal Components Analysis of the Samples in the Discovery Set**

Principal components analysis (PCA) plot of PC1 & PC2 based on all transcripts and samples in the discovery cohort after background adjustment and normalization. No sample was removed from the analysis at this stage. A confidence ellipse has been calculated for the population mean and is shown below (99%).



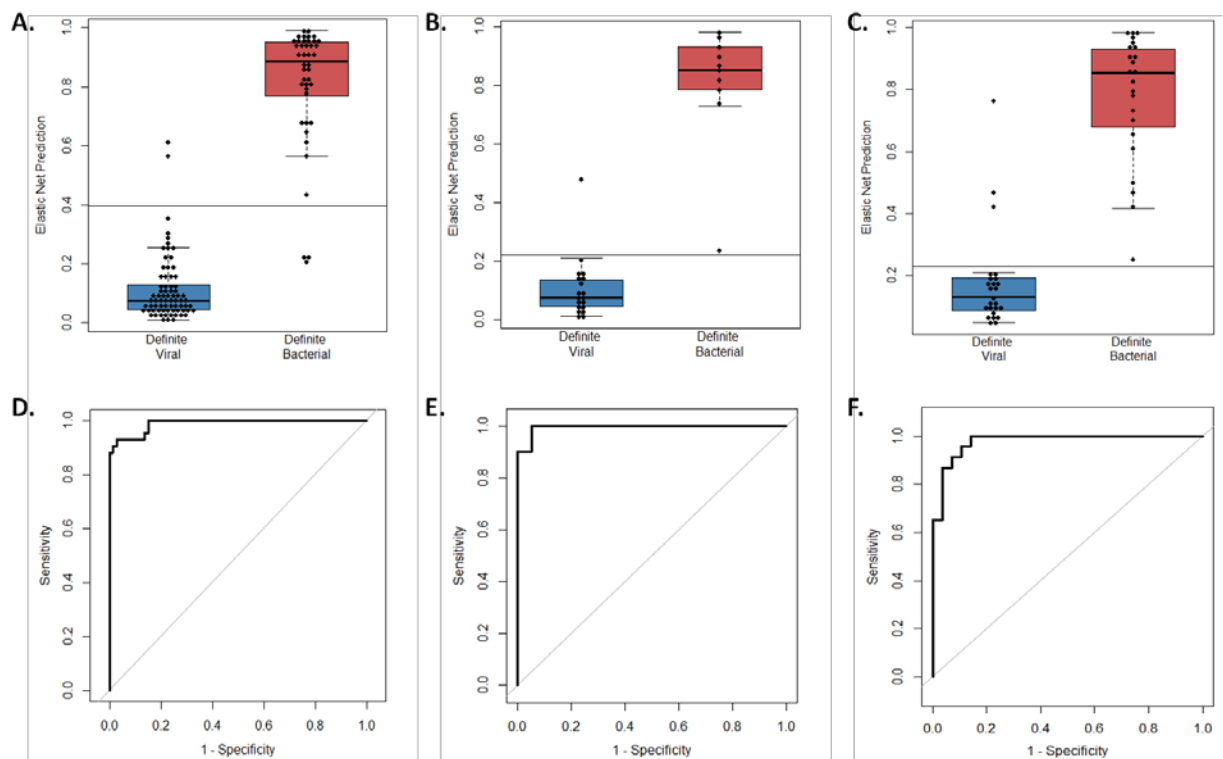
Number of arrays for each sample are: Viral n=92, Probable Viral n=5, Unknown n=49, Probable Bacterial n=42, Bacterial n=52.





**eFigure 3. Elastic Net Prediction Value and Receiver Operator Characteristic Curves Based on the 38-Transcript Signature Applied to the Definite Bacterial and Viral Groups**

Classification performance and Receiver Operating Characteristic (ROC) curve, based on the 38-transcript signature, applied to the Definite Bacterial and Viral groups of the 80% training set (A & D), the 20% test set (B & E) and the IRIS validation dataset (C & F). Sensitivity, specificity and AUC are reported in eTable 3. Boxes show median with 25<sup>th</sup> and 75<sup>th</sup> quartiles; whiskers (defined by “range” in *boxplot* function in R) can extend no more than 1 times the interquartile range. The elastic net prediction value (the outcome variable Y obtained from fitting the elastic net model) can range from 0 (indicating viral infection) to 1 (indicating bacterial infection).

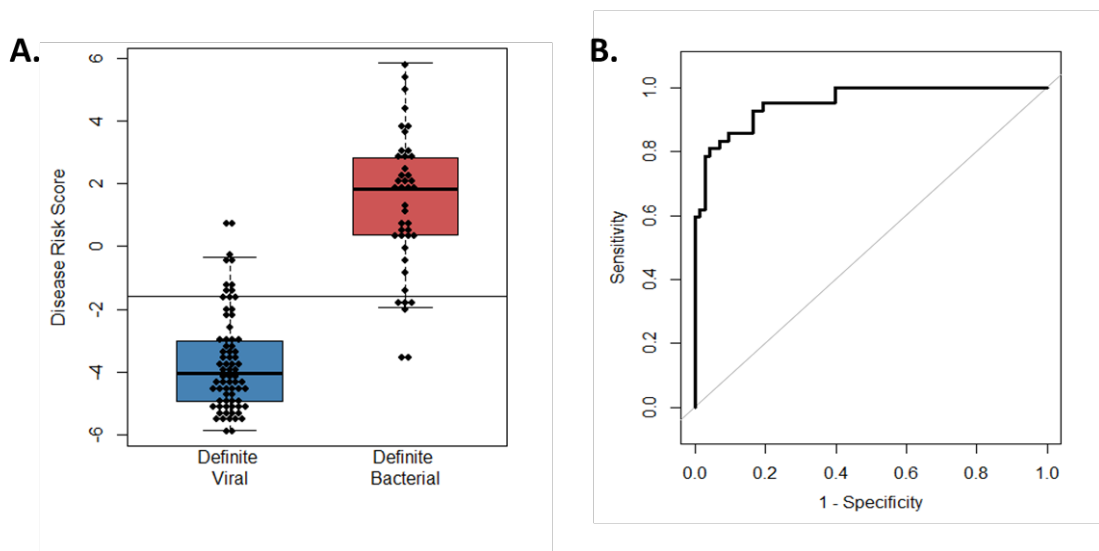


Patients in the training set: Definite Bacterial n=42, Definite Viral n=92. Patients in the test set: Definite Bacterial n=10, Definite Viral n=19. Patients in IRIS validation dataset: Definite Bacterial n=23, Definite Viral n=28.

**eFigure 4. Disease Risk Scores and Receiver Operator Characteristic Curves Based on the 2-Transcript Signature Applied to Training Set**

Classification performance (A) and Receiver Operating Characteristic (ROC) curve (B), based on the 2-transcript Disease Risk Score signature (the combination of *IFI44L* and *FAM89A*), applied to the Definite Bacterial and Viral groups of the 80% training set. Sensitivity, specificity and Area Under the Curve are reported in eTable 3. Boxes show median with 25<sup>th</sup> and 75<sup>th</sup> quartiles; whiskers, plotted using 'boxplot' in R, extend  $\leq 1$  times the interquartile range. The horizontal DRS threshold line separates patients predicted as bacterial (above) or viral (below the threshold). The threshold is determined by the point on the ROC curve that maximizes sensitivity and specificity (see Supplementary Statistical Methods).

**Training Dataset**



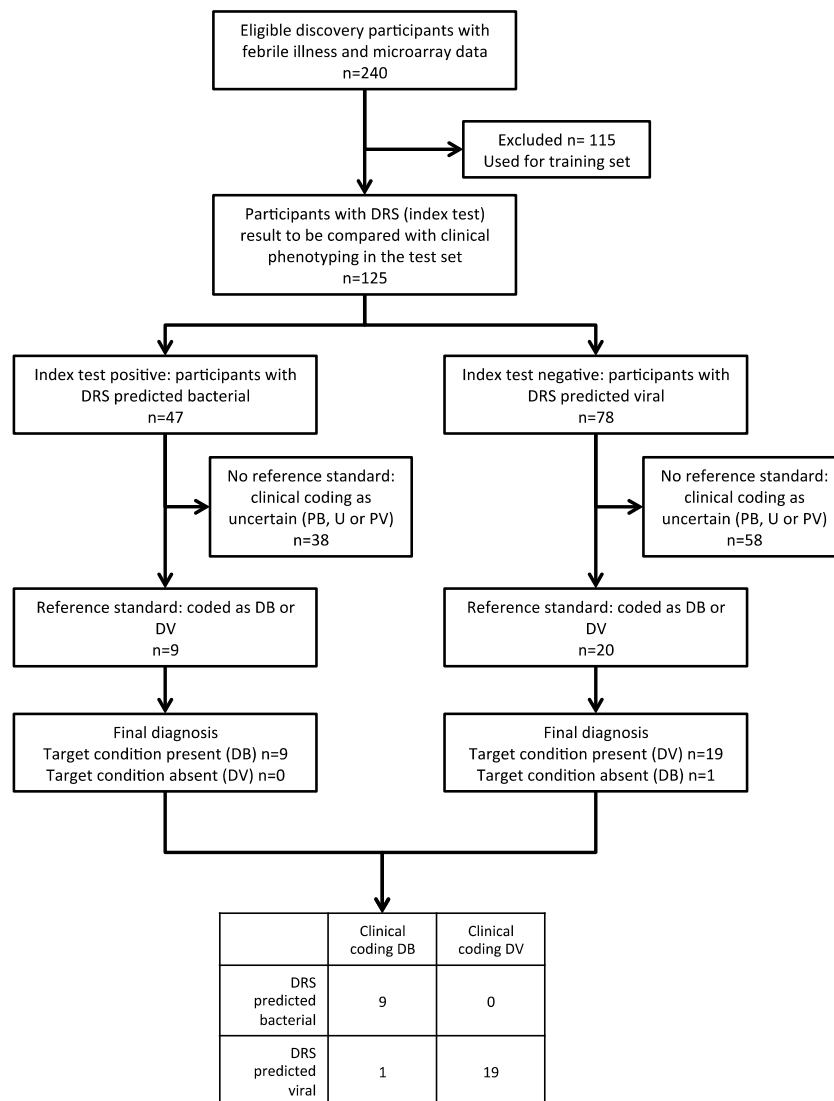
Patients in the training set: Definite Bacterial n=42, Definite Viral n=92.

**eFigure 5. STARD Flow Diagrams and Assessment of Diagnostic Test Accuracy**

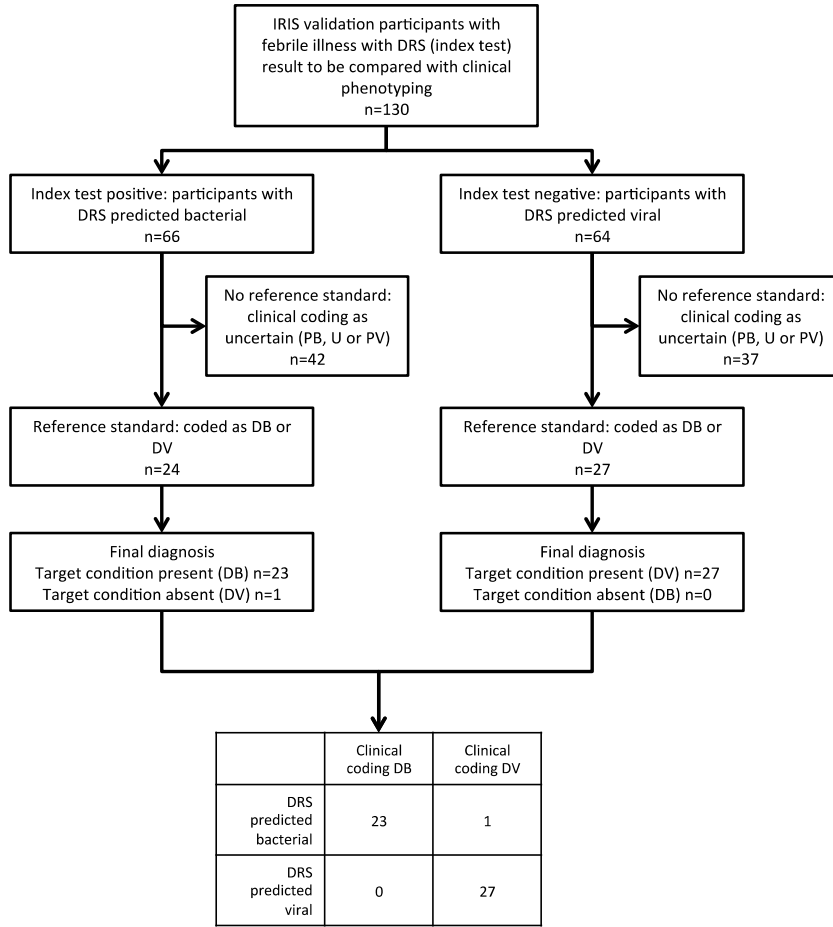
STARD flow diagram for assessment of diagnostic test accuracy in the test set (A) and validation set (B), including a 2x2 table of results comparing performance of the 2-transcript Disease Risk Score (DRS) against the clinical coding as bacterial or viral infection.

DB – Definite Bacterial; DV – Definite Viral; PB – Probable Bacterial; U – Unknown Bacterial or Viral; PV – Probable Viral

A

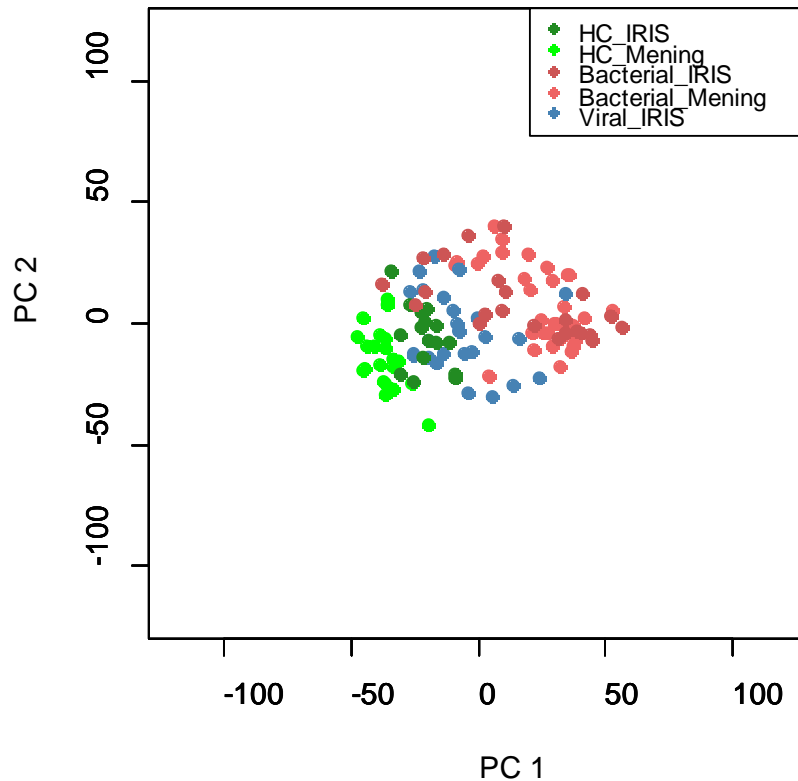


B



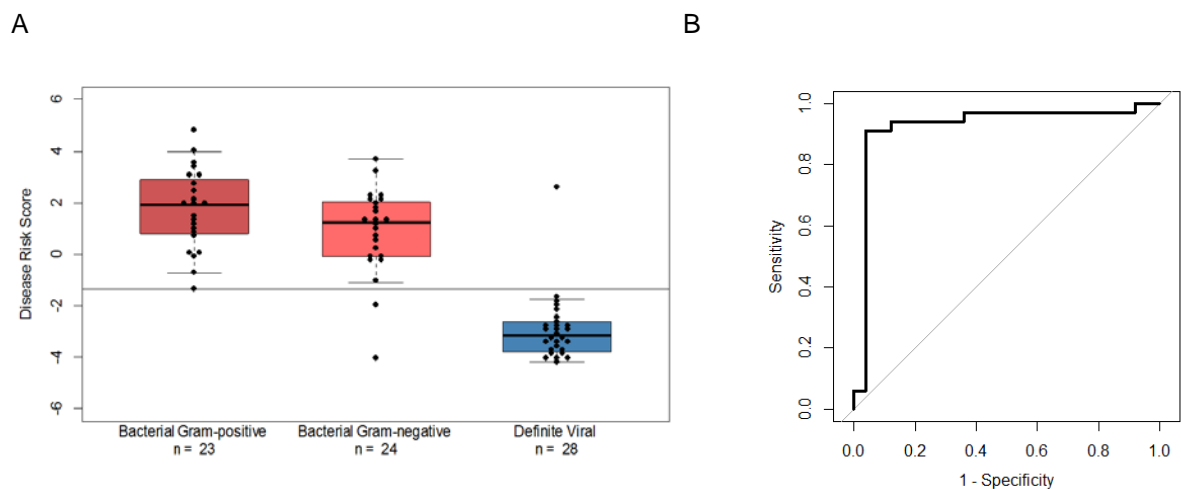
**eFigure 6. Principal Component Analysis of Meningococcal and IRIS Validation Samples After Merging With ComBat**

The two-transcript Disease Risk Score classifier was applied on external data, and its ability to discriminate between bacterial and non-bacterial patients was assessed. In the case of the meningococcal validation data set, there were no comparator non-bacterial patients, and in order to estimate the accuracy of the Disease Risk Score signature, we employed the viral group of the IRIS validation dataset. The two datasets were merged using the ComBat method to remove non-biological experimental variation, using the healthy controls from both datasets as reference. The Principal components analysis plot of the merged dataset indicates successful removal of the batch effects. The healthy controls from the IRIS dataset (*HC\_IRIS* n=16) and the healthy controls from the meningococcal dataset (*HC\_Mening* n=21) are shown lying adjacent, as well as the bacterial patients from both datasets (*Bacterial\_IRIS* n=23 and *Bacterial\_Mening* n=24). The viral patients of the IRIS dataset are shown in blue (*Viral\_IRIS* n=28). The 1<sup>st</sup> principal component was found to capture the differences in gene expression by infection status.



**eFigure 7. Disease Risk Scores and Receiver Operator Characteristic Curves Based on the 2-Transcript Signature Applied to Children With Gram-Negative and Gram-Positive Infection**

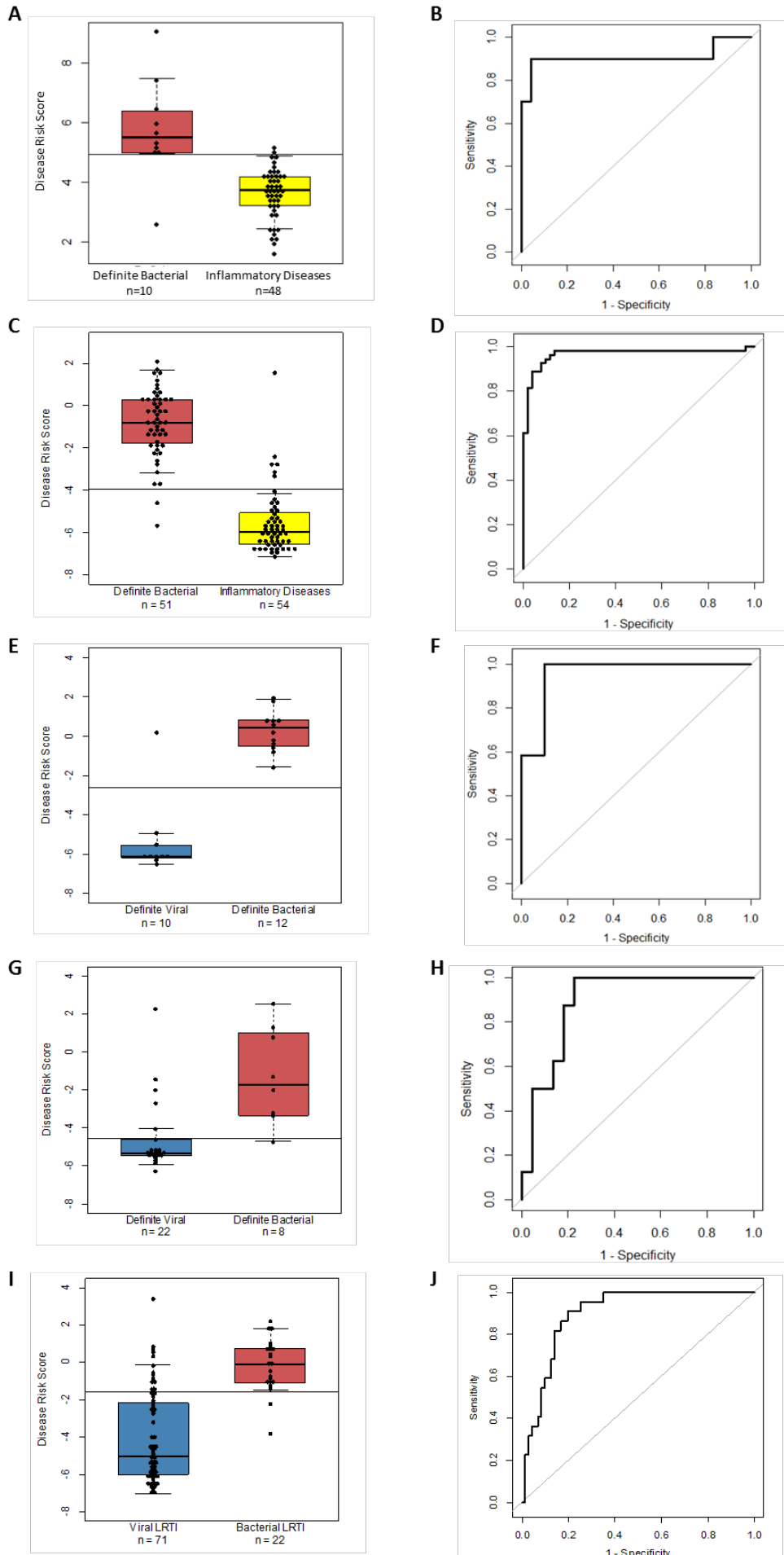
The classification performance (A) and Receiver Operating Characteristic (ROC) curve (B), based on the 2-transcript Disease Risk Score signature (the combination of *IFI44L* and *FAM89A*), applied to the gram-positive (IRIS validation), gram-negative (IRIS and meningococcal validation), and viral (IRIS validation) groups of the merged datasets. Boxes show median with 25<sup>th</sup> and 75<sup>th</sup> quartiles; whiskers, plotted using 'boxplot' in R, extend  $\leq 1$  times the interquartile range. The horizontal DRS threshold line separates patients predicted as bacterial (above) or viral (below the threshold). It is determined by the point on the ROC curve that maximizes sensitivity and specificity (see Supplementary Statistical Methods). Sensitivity, specificity and Area Under the Curve are reported in eTable 6, based on discrimination of gram-negative infection and viral infection. The bacterial gram-positive group is shown for illustrative purposes.



**eFigure 8. Disease Risk Scores and Receiver Operator Characteristic Curves Based on the 2-Transcript Signature Applied to Additional Validation Datasets**

The classification performance and Receiver Operating Characteristic (ROC) curve based on the 2-transcript Disease Risk Score signature (the combination of *IFI44L* and *FAM89A*) applied to the inflammatory validation groups Juvenile Idiopathic arthritis (JIA) and Henoch Schönlein Purpura (HSP) (A, B); and to 4 external published datasets: bacterial and inflammatory patients with systemic lupus erythematosus (C, D) [13]; bacterial and viral patients from the Ramilo *et al* study (E, F) [11]; bacterial and viral patients from the Hu *et al* study (G, H) [12]; and bacterial and viral patients from the Suarez *et al* study (I, J) [14]. Boxes show median with 25<sup>th</sup> and 75<sup>th</sup> quartiles; whiskers, plotted using 'boxplot' in R, extend  $\leq 1$  times the interquartile range. The horizontal DRS threshold line separates patients predicted as bacterial (above) or viral (below the threshold). It is determined by the point on the ROC curve that maximizes sensitivity and specificity (see Supplementary Statistical Methods). Sensitivity, specificity and Area Under the Curve are reported in eTable 6.

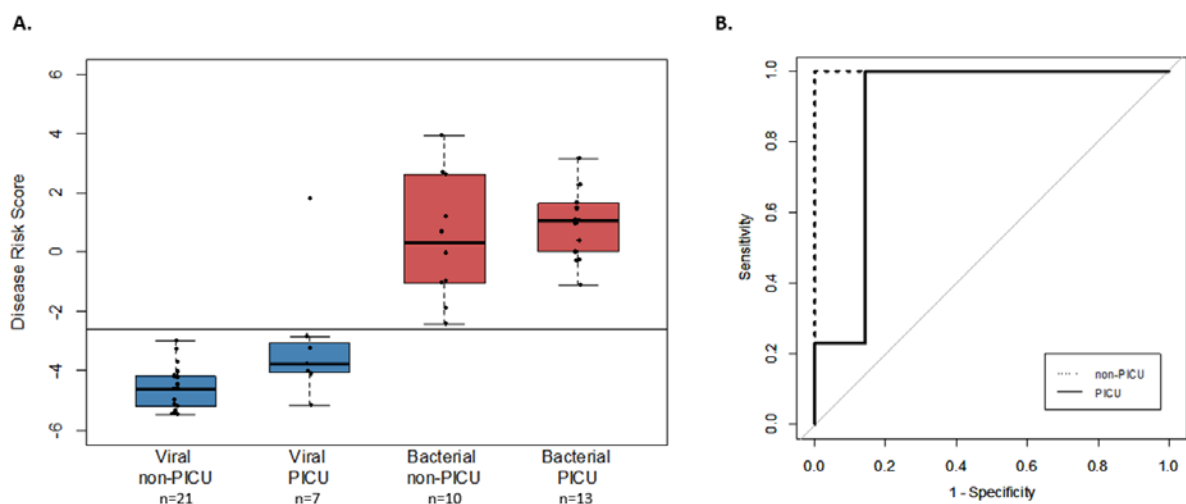




© 2016 American Medical Association. All rights reserved.

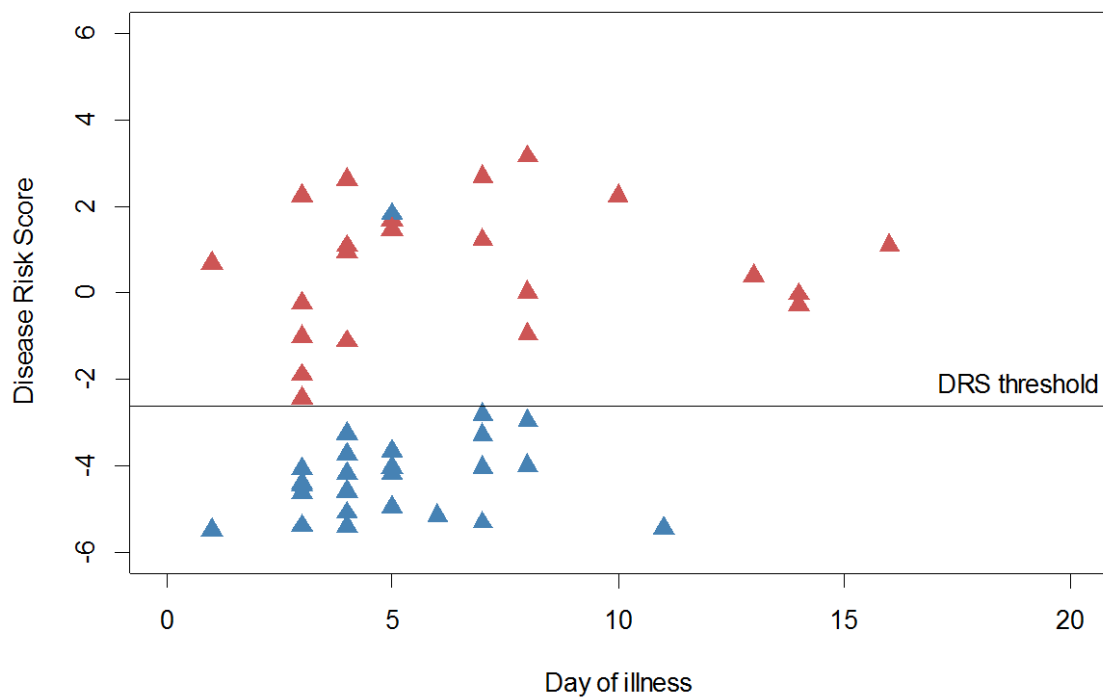
**eFigure 9. Performance of the Disease Risk Score in Relation to Severity of Illness in the IRIS Validation Set**

In order to investigate whether the severity of illness influenced the performance of the 2-transcript classifier, we analyzed the Disease Risk Score (DRS) values (the combined *IFI44L* and *FAM89A* expression values) in the definite Viral and definite Bacterial groups by need for admission to the pediatric intensive care unit (PICU) during their illness (as shown in Figure 4B). The horizontal DRS threshold line separates patients predicted as bacterial (above the line) or viral (below the line) (A). The 2-transcript DRS classified patients as bacterial or viral irrespective of their requirement for intensive care. The classification performance and Receiver Operating Characteristic (ROC) curve, based on the 2-transcript DRS signature is shown for patients requiring intensive care (solid line) or not requiring intensive care (dotted line) (B).



**eFigure 10. Performance of the Disease Risk Score in Relation to Day of Illness in the IRIS Validation Set**

In order to investigate whether the duration of illness influenced performance of the 2-transcript classifier, Disease Risk Score (DRS) values were plotted relative to the patient-reported day of illness (including symptomatic days before hospital admission) at the time of blood sampling. The horizontal DRS threshold line separates patients predicted as bacterial (above the line) and viral (below the line) (as shown on Figure 4B). Red triangles denote Definite Bacterial patients; blue triangles denote Definite Viral patients. There was no correlation of illness day with DRS. The plot does not include a single patient with a long illness.



**eTable 1. Demographic and Clinical Features of the Validation Groups**

	<b>Meningococcal Disease<sup>a</sup></b>	<b>Juvenile Idiopathic Arthritis<sup>b</sup></b>	<b>Henoch-Schönlein purpura<sup>c</sup></b>
Number of patients	24	30	18
Age - mo. median (IQR)	23 (17-35)	163 (124-187)	56 (43-81)
Male, No. (%)	16 (66%)	11 (37%)	9 (50%)
White ethnicity - no. (%)	24/24 (100%)	27/30 (90%)	4/18 (22%)
Days from symptoms - median (IQR)	1(1-1)	n/a	3.5 (2-6)
Intensive care, No. (%)	24 (100%)	0	0
Deaths, No. (%)	3 (12.5%)	0	0
CRP (mg/dl) - median (IQR)	6.8 (3.4-10)	0.1 (0.0-0.2)	2.2 (0.8-2.4)
Neutrophil %: median (IQR)	71 (56-83)	51 (45-57)	60 (45-68)
Lymphocyte %: median (IQR)	23 (12-53)	37 (33-45)	26 (16-34)
Monocyte %: median (IQR)	ND	7 (6-8)	7 (5-8)

<sup>a</sup> sample size for data fields: % neutrophil n=20, % lymphocyte n=12, CRP n=22.

<sup>b</sup> sample size for JIA (juvenile idiopathic arthritis) disease categories: enthesitis-related arthritis n=6, extended oligoarthritis n=4, persistent oligoarthritis n=4, polyarthritis rheumatoid factor (RF)-negative n=12, polyarthritis RF-positive n=1, psoriatic n=3. Sample size for data fields: % neutrophil n=27, % lymphocyte n=27, % monocyte n=27

<sup>c</sup> HSP (Henoch-Schönlein purpura). Sample size for data fields: % neutrophil n=15, % monocyte n=15, CRP n=8

**eTable 2. Viral and Bacterial Causative Pathogens in Patients in the Definite Bacterial and Viral Groups in the Discovery and IRIS Validation Cohorts**

	Definite Viral		Definite Bacterial	
	Discovery (n)	Validation (n)	Discovery (n)	Validation (n)
<b>Viral causative pathogen</b>				
Adenovirus	23	2		
Influenza A or B	23	13		
RSV	27	10		
Other	19	3		
<b>Bacterial causative pathogen</b>				
<i>S.pneumoniae</i>			10	15
<i>S.aureus</i>			2	2
<i>S.pyogenes</i>			10	5
Group B streptococcus			4	
<i>E.coli</i>			2	
<i>N.meningitidis</i>			17	24
<i>Enterococcus</i>			1	
<i>Kingella</i>			1	
<i>H.influenzae</i>			1	
<i>Pseudomonas</i> spp			3	
<i>Stenotrophomonas</i>			1	
<i>Klebsiella</i>				1
<b>Total number of patients</b>	92	28	52	47

**eTable 3. 38-Transcript Signature for Distinguishing Bacterial From Viral Infection**

Array ID	Elastic net coefficient	Transcript ID	Official Symbol (HGNC)	Definition	Definite Bacterial vs. Definite Viral		Definite Bacterial vs Healthy Control		Definite Viral vs Healthy Control	
					log <sub>2</sub> FC	q-value <sup>a</sup>	log <sub>2</sub> FC	q-value <sup>a</sup>	log <sub>2</sub> FC	q-value <sup>a</sup>
3990170	-0.18	ILMN_17548	<i>IFI27</i>	Homo sapiens interferon, alpha-inducible protein 27, transcript variant 2, mRNA.	-4.32	4.78E-21	1.08	7.06E-02	5.40	3.15E-23
3870338*	-0.02	ILMN_9752	<i>IFI44L</i>	Homo sapiens interferon-induced protein 44-like, mRNA.	-3.79	1.36E-22	-1.11	1.98E-02	2.68	4.45E-10
2000148	-0.06	ILMN_1751	<i>IFIT1</i>	Homo sapiens interferon-induced protein with tetratricopeptide repeats 1, transcript variant 2, mRNA.	-3.49	2.90E-20	-1.15	1.48E-02	2.35	3.89E-08
3360343	-0.03	ILMN_37168	<i>RSAD2</i>	Homo sapiens radical S-adenosyl methionine domain containing 2, mRNA.	-3.28	5.14E-19	-0.75	1.48E-01	2.53	2.11E-09
6510170	-0.04	ILMN_22925	<i>IFIT3</i>	Homo sapiens interferon-induced protein with tetratricopeptide repeats 3, mRNA.	-2.66	2.47E-16	-0.90	3.77E-02	1.77	3.25E-06
520408	-0.04	ILMN_1944	<i>IFIT3</i>	Homo sapiens interferon-induced protein with tetratricopeptide repeats 3, mRNA.	-2.56	1.20E-16	-0.94	1.90E-02	1.62	7.09E-06
1440615	-0.05	ILMN_27303	<i>OTOF</i>	Homo sapiens otoferlin, transcript variant 4, mRNA.	-2.53	1.73E-14	0.08	9.22E-01	2.61	4.01E-11
26	-0.07	ILM	<i>IFIT2</i>	Homo sapiens interferon-induced protein with tetratricopeptide	-2.40	7.83E-	-1.15	1.22E-	1.25	2.33E-

00747		N_28123		repeats 2, mRNA.		17		03		04
5700725	-0.05	ILM_N_27754	<i>EPSTI1</i>	Homo sapiens epithelial stromal interaction 1 (breast), transcript variant 2, mRNA.	-2.23	1.90E-20	-0.55	8.77E-02	1.69	5.76E-10
2030309	-0.05	ILM_N_15074	<i>SERPIN_G1</i>	Homo sapiens serpin peptidase inhibitor, clade G (C1 inhibitor), member 1, transcript variant 2, mRNA.	-2.19	4.14E-12	-0.18	7.94E-01	2.01	9.82E-08
1090390	-0.04	ILM_N_2717	<i>OAS1</i>	Homo sapiens 2',5'-oligoadenylate synthetase 1, 40/46kDa, transcript variant 3, mRNA.	-2.13	2.10E-18	-0.27	5.13E-01	1.86	5.60E-11
5090215	-0.17	ILM_N_13978	<i>IFI6</i>	Homo sapiens interferon, alpha-inducible protein 6, transcript variant 3, mRNA.	-1.55	1.23E-18	-0.41	8.55E-02	1.14	1.53E-08
620544	-0.13	ILM_N_5312	<i>HLA-DRB6</i>	Homo sapiens major histocompatibility complex, class II, DR beta 6 (pseudogene), non-coding RNA.	-1.42	8.94E-05	-1.93	2.02E-05	-0.51	4.40E-01
6980192	-0.02	ILM_N_19775	<i>HBZ</i>	Homo sapiens hemoglobin, zeta, mRNA.	-1.33	2.85E-03	-0.43	5.97E-01	0.90	1.69E-01
1030100	-0.22	ILM_N_89157	<i>HS.386275</i>	cl02h05.z1 Hembase; Erythroid Precursor Cells (LCB:cl library) Homo sapiens cDNA clone cl02h05 5, mRNA sequence	-1.31	2.84E-14	-0.42	8.24E-02	0.89	1.19E-05
2120079	-0.11	ILM_N_168435	<i>EIF2AK2</i>	Homo sapiens eukaryotic translation initiation factor 2-alpha kinase 2, mRNA.	-1.24	1.25E-12	-0.08	8.48E-01	1.16	2.55E-08
378045	-0.01	ILM_N_5646	<i>IFIT1L</i>	Homo sapiens interferon-induced protein with tetratricopeptide repeats 1-like, mRNA.	-1.18	5.13E-03	0.29	7.22E-01	1.47	3.89E-03

2										
33 60 61 5	-0.04	ILM N_1 8288	<i>FCER1A</i>	Homo sapiens Fc fragment of IgE, high affinity I, receptor for; alpha polypeptide, mRNA.	-1.13	6.50E-07	-2.80	2.28E-19	-1.66	2.24E-09
15 03 15	-0.18	ILM N_9 078	<i>C21ORF7</i>	Homo sapiens chromosome 21 open reading frame 7, mRNA.	-1.12	3.53E-11	-1.11	1.18E-07	0.01	9.86E-01
69 40 08 6	-0.02	ILM N_2 1264	<i>GYPE</i>	Homo sapiens glycophorin E, transcript variant 1, mRNA.	-1.11	2.37E-03	0.33	6.31E-01	1.44	1.06E-03
37 80 18 7	-0.06	ILM N_2 7651	<i>GYPB</i>	Homo sapiens glycophorin B (MNS blood group), mRNA.	-1.09	3.03E-03	0.46	4.56E-01	1.55	3.76E-04
44 80 73 0	-0.12	ILM N_2 819	<i>HBM</i>	Homo sapiens hemoglobin, mu, mRNA.	-1.02	1.03E-04	0.08	8.98E-01	1.10	6.73E-04
41 50 60 0	-0.19	ILM N_1 4704	<i>EIF1AY</i>	Homo sapiens eukaryotic translation initiation factor 1A, Y-linked, mRNA.	-1.00	1.61E-02	0.24	7.73E-01	1.24	1.43E-02
10 10 54 6	-0.02	ILM N_4 3805	<i>LOC649143</i>	PREDICTED: Homo sapiens similar to HLA class II histocompatibility antigen, DRB1-9 beta chain precursor (MHC class I antigen DRB1*9) (DR-9) (DR9), transcript variant 2, mRNA.	-0.95	2.37E-04	-1.33	3.83E-05	-0.37	4.16E-01
14 50 35 8	-0.02	ILM N_9 543	<i>HBD</i>	Homo sapiens hemoglobin, delta, mRNA.	-0.69	2.79E-02	-0.44	3.66E-01	0.26	6.76E-01
46 70 32 7	-0.11	ILM N_2 8646	<i>FBXO7</i>	Homo sapiens F-box protein 7, transcript variant 2, mRNA.	-0.65	1.09E-02	-0.65	5.11E-02	0.00	9.98E-01
55 50	0.07	ILM N_2	<i>KCNMA1</i>	Homo sapiens potassium large conductance calcium-activated channel, subfamily M, alpha member 1, transcript variant 2,	0.95	2.01E-09	1.13	1.29E-08	0.18	5.69E-01



45 2		4236		mRNA.						
75 50 06 6	0.00	ILM N_1 7301 6	<i>MERTK</i>	Homo sapiens c-mer proto-oncogene tyrosine kinase, mRNA.	1.04	3.04E-09	1.59	1.53E-12	0.55	1.85E-02
28 10 76 7	0.45	ILM N_2 3396	<i>EBI3</i>	Homo sapiens Epstein-Barr virus induced 3, mRNA.	1.10	8.79E-13	0.81	1.71E-05	- 0.28	2.41E-01
40 40 24 2*	0.24	ILM N_2 1686	<i>FAM89A</i>	Homo sapiens family with sequence similarity 89, member A, mRNA.	1.21	2.97E-14	1.56	1.42E-14	0.34	1.37E-01
38 30 73 5	0.03	ILM N_9 777	<i>UPB1</i>	Homo sapiens ureidopropionase, beta, mRNA.	1.23	5.27E-13	1.67	2.14E-14	0.43	6.51E-02
74 00 74 7	0.22	ILM N_2 1686	<i>FAM89A</i>	Homo sapiens family with sequence similarity 89, member A, mRNA.	1.26	7.65E-14	1.65	1.13E-14	0.40	9.38E-02
25 10 35 6	0.02	ILM N_1 2984	<i>EMR1</i>	Homo sapiens egf-like module containing, mucin-like, hormone receptor-like 1, mRNA.	1.33	1.50E-11	1.32	6.00E-08	- 0.01	9.91E-01
38 50 64 7	0.14	ILM N_1 3735 6	<i>PTPN20</i>	PREDICTED: Homo sapiens protein tyrosine phosphatase, non-receptor type 20, mRNA.	1.35	1.88E-11	1.98	2.35E-14	0.63	1.77E-02
38 30 76 2	0.04	ILM N_3 0233	<i>TMEM119</i>	Homo sapiens transmembrane protein 119, mRNA.	1.35	1.76E-08	2.10	8.55E-12	0.74	2.07E-02
21 40 70 7	0.08	ILM N_2 8045	<i>SLPI</i>	Homo sapiens secretory leukocyte peptidase inhibitor, mRNA.	1.84	2.44E-12	2.78	4.34E-16	0.94	4.79E-03

15 10 42 4	0.06	ILM N_2 3476	<i>S100P</i>	Homo sapiens S100 calcium binding protein P, mRNA.	2.35	1.39E- 16	2.91	6.99E- 16	0.56	1.85E- 01
10 50 16 8	0.03	ILM N_1 3685	<i>PI3</i>	Homo sapiens peptidase inhibitor 3, skin-derived, mRNA.	2.58	4.52E- 10	0.77	2.39E- 01	- 1.82	3.76E- 04

\* Transcripts that comprise the 2-transcript DRS signature.

HGNC = HUGO Gene Nomenclature Committee, FC = Fold Change.

<sup>a</sup>This is the P-value corrected for false discovery, using Benjamini-Hochberg method [15], for the difference in expression between the 2 comparator groups for each transcript using a moderated t-test in R using *limma* [16].

**eTable 4. Diagnostic Performance of the Bacterial vs. Viral 38-Transcript Elastic Net and Disease Risk Score 2-Transcript Signatures in the Training, Test and IRIS Validation Datasets**

	Training Set	Test Set	IRIS Validation Set
<b>Definite Bacterial patients (n)</b>	42	10	23
<b>Definite Viral patients (n)</b>	73	19	28
<b>38-transcript signature derived from elastic net model</b>			
<b>Area under ROC curve</b>	98.9	99.5	97.8
<b>(95% CI)</b>	(97.4 - 99.9)	(96.8 - 100.0)	(93.8 - 100.0)
<b>Sensitivity %</b>	92.9	100.0	100.0
<b>(95% CI)</b>	(83.3 - 100.0)	(69.2 - 100.0)	(85.2 - 100.0)
<b>Specificity %</b>	97.3	94.7	85.71
<b>(95% CI)</b>	(93.2 - 100.0)	(84.2 - 100.0)	(71.4 - 96.4)
<b>2-transcript signature derived from Disease Risk Score model</b>			
<b>Area under ROC curve</b>	95.5	96.3	97.4
<b>(95% CI)</b>	(91.8 - 98.4)	(87.4 - 100.0)	(91.2 - 100.0)
<b>Sensitivity %</b>	85.7	90.0	100.0
<b>(95% CI)</b>	(73.8 - 95.2)	(70.0 - 100.0)	(85.2 - 100.0)
<b>Specificity %</b>	84.9	100	96.4
<b>(95% CI)</b>	(76.7 - 91.8)	(82.4 - 100.0)	(89.3 - 100.0)

ROC = Receiver Operating Characteristic

**Table 5. Gene Ontology (GO) Biological Process Terms Analysis**

GO Term (Biological Process)	Number of genes mapped		Expected value <sup>c</sup>	Over (+) or under (-) representation <sup>d</sup>	Fold enrichment <sup>e</sup>	P-value <sup>f</sup>	Genes associated with the GO Term
	Background Reference <sup>a</sup>	Signature <sup>b</sup>					
<b>Cellular response to interferon-alpha</b> (GO:0035457)	9	3	0.01	+	> 5	3.09E-03	<i>IFIT2; OAS1; IFIT3</i>
<b>Response to interferon-alpha</b> (GO:0035455)	18	4	0.03	+	> 5	1.53E-04	<i>IFIT2; OAS1; IFIT3; EIF2AK2</i>
<b>Oxygen transport</b> (GO:0015671)	15	3	0.02	+	> 5	1.42E-02	<i>HBD; HBM; HBZ</i>
<b>Gas transport</b> (GO:0015669)	19	3	0.03	+	> 5	2.88E-02	<i>HBD; HBM; HBZ</i>
<b>Negative regulation of viral genome replication</b> (GO:0045071)	46	5	0.07	+	> 5	7.86E-05	<i>SLPI; IFIT1; OAS1; RSAD2; EIF2AK2</i>
<b>Type I interferon signalling pathway</b> (GO:0060337)	68	7	0.1	+	> 5	9.68E-08	<i>IFIT2; IFIT1; OAS1; IFI27; RSAD2; IFI6; IFIT3</i>
<b>Cellular response to type I interferon</b> (GO:0071357)	68	7	0.1	+	> 5	9.68E-08	<i>IFIT2; IFIT1; OAS1; IFI27; RSAD2; IFI6; IFIT3</i>
<b>Response to type I interferon</b> (GO:0034340)	69	7	0.11	+	> 5	1.07E-07	<i>IFIT2; IFIT1; OAS1; IFI27; RSAD2; IFI6; IFIT3</i>
<b>Regulation of viral genome replication</b> (GO:0045069)	70	5	0.11	+	> 5	6.25E-04	<i>SLPI; IFIT1; OAS1; RSAD2; EIF2AK2</i>
<b>Negative regulation of viral life cycle</b>	84	5	0.13	+	> 5	1.53E-	<i>SLPI; IFIT1; OAS1; RSAD2; EIF2AK2</i>

(GO:1903901)						03	
<b>Negative regulation of viral process</b> (GO:0048525)	87	5	0.13	+	> 5	1.8 2E- 03	<i>SLPI; IFIT1; OAS1; RSAD2; EIF2AK2</i>
<b>Defence response to virus</b> (GO:0051607)	159	7	0.24	+	> 5	3.3 6E- 05	<i>IFIT2; IFIT1; OAS1; IFI44L; RSAD2; EIF2AK2; IFIT3</i>
<b>Negative regulation of multi-organism process</b> (GO:0043901)	150	5	0.23	+	> 5	2.5 9E- 02	<i>SLPI; IFIT1; OAS1; RSAD2; EIF2AK2</i>
<b>Response to virus</b> (GO:0009615)	240	7	0.37	+	> 5	5.5 1E- 04	<i>IFIT2; IFIT1; OAS1; IFI44L; RSAD2; EIF2AK2; IFIT3</i>
<b>Defence response to other organism</b> (GO:0098542)	371	8	0.57	+	> 5	5.6 9E- 04	<i>SLPI; IFIT2; IFIT1; OAS1; IFI44L; RSAD2; EIF2AK2; IFIT3</i>
<b>Immune effector process</b> (GO:0002252)	447	8	0.69	+	> 5	2.3 3E- 03	<i>IFIT2; IFIT1; OAS1; IFI44L; RSAD2; EIF2AK2; SERPING1; IFIT3</i>
<b>Cytokine-mediated signalling pathway</b> (GO:0019221)	487	8	0.75	+	> 5	4.4 4E- 03	<i>IFIT2; IFIT1; OAS1; IFI27; RSAD2; IFI6; IFIT3; EBI3</i>
<b>Cellular response to cytokine stimulus</b> (GO:0071345)	632	8	0.97	+	> 5	3.0 7E- 02	<i>IFIT2; IFIT1; OAS1; IFI27; RSAD2; IFI6; IFIT3; EBI3</i>
<b>Response to cytokine</b> (GO:0034097)	730	9	1.12	+	> 5	8.4 0E- 03	<i>IFIT2; IFIT1; OAS1; IFI27; RSAD2; IFI6; EIF2AK2; IFIT3; EBI3</i>
<b>Innate immune response</b> (GO:0045087)	1012	10	1.56	+	> 5	1.3 8E- 02	<i>IFIT2; IFIT1; OAS1; IFI27; RSAD2; IFI6; EIF2AK2; SERPING1; IFIT3; FCER1A</i>
<b>Immune response</b> (GO:0006955)	1430	14	2.2	+	> 5	5.8 2E- 05	<i>SLPI; IFIT2; IFIT1; EMR1; OAS1; IFI44L; IFI27; RSAD2; IFI6; EIF2AK2; IFIT3; SERPING1; EBI3; FCER1A</i>
<b>Defence response</b> (GO:0006952)	1507	12	2.32	+	> 5	9.1 9E- 03	<i>SLPI; IFIT2; IFIT1; OAS1; IFI27; IFI44L; RSAD2; IFI6; EIF2AK2; SERPING1; IFIT3; FCER1A</i>

<b>Immune system process</b> (GO:0002376)	2163	16	3.33	+	4.81	1.6 7E- 04	<i>SLPI; IFIT2; HBZ; IFIT1; EMR1; MERTK; OAS1; IFI44L; IFI27; RSAD2; IFI6; EIF2AK2; IFIT3; SERPING1; EBI3; FCER1A;</i>
<b>Unclassified</b> (Unclassified)	4272	6	6.57	-	0.91	0.0 0E+ 00	<i>GYPB; EPSTI1; FAM89A; MAP3K7CL; GYPE; IFIT1B</i>

Overrepresentation test for the genes in the 38-transcript signature for the GO: biological process Homo sapiens terms using the PANTHER Pathway resource (Bonferroni corrected) [17],[18].

<sup>a</sup> number of genes mapped to GO terms when using the background reference dataset of *Homo Sapiens*. The total number of genes in this dataset is 20814.

<sup>b</sup> number of genes mapped to GO terms when using genes in the 38-transcript signature. The total number of genes in the signature is 36.

<sup>c</sup> number of genes expected to be in signature for this category, based on the background reference dataset.

<sup>d</sup> + indicates an over-representation of the GO term in the signature, - indicates an under-representation of the GO term in the signature.

<sup>e</sup> GO term over-represented if >1, under-represented if <1

<sup>f</sup> Probability that the number of genes from the signature in the GO term occurred randomly.

**eTable 6. Additional Validation and External Microarray Datasets**

Overview of the gene expression microarray datasets used for assessment of the 2-transcript Disease Risk Score signature. Study and experimental details, as well as the metrics for classification accuracy (i.e. Sensitivity, Specificity and Area Under the Curve (AUC) with 95% Confidence Intervals [CI]) are shown.

1 <sup>st</sup> group	2 <sup>nd</sup> group	Gene Expression Omnibus accession	Reference	Age (years)	Platform	Results after application of the 2-transcript DRS signature			
						Sensitivity % (95%CI)	Specificity % (95%CI)	AUC % (95%CI)	Related eFigure
Meningococcal validation: 24 children	Viral group of the IRIS validation set (after data merging)	GSE80496	Unpublished	<3	Illumina Ref8-V3	91.7 (79.2-100)	96.0 (88.0-100)	92.6 (81.3-100)	eFig 6
Inflammatory validation: 30 JIA & 18 HSP	20% Discovery Bacterial set (after data merging)	GSE80412	Unpublished	<18	Illumina HT12-V4	90.0 (70.0-100)	95.8 (89.6-100)	90.8 (73-100)	eFig 7
48 bacterial: (S.aureus, streptococcus)	31 Pediatric SLE	GSE22098	Berry M (2010) [13]	<17	Illumina HT12-V3	93.5 (83.9-100)	96.1 (90.2-100)	96.6 (91.9-100)	eFig 7
12 bacterial (S.pneumoniae, S.aureus)	10 viral (Influenza A and B)	GSE6269 – GPL570	Ramilo O (2007)[11]	<16	Affymetrix	100 (73.5-100)	90 (70-100)	96 (85-100)	eFig 7
8 bacterial – mixed gram positive & gram negative	22 viral – mixed adenovirus, HHV6, enterovirus	GSE40396	Hu X (2013) [12]	<3	Illumina HT12-V4	100 (63.1-100)	77.3 (59.1-95.5)	89.2 (75.6-98.3)	eFig 7

15 bacterial LTRI	64 Viral LTRI	GSE60244	Suarez N (2015) [14]	Adults	Illumina HT12-V4	90.1 (77.3-100)	80.3 (70.4-88.7)	89.8 (83.4-95.5)	eFig 7
-------------------	---------------	----------	----------------------	--------	------------------	-----------------	------------------	------------------	--------

DRS Disease Risk Score, JIA Juvenile Idiopathic arthritis, HSP Henoch Schönlein Purpura, LTRI Lower respiratory tract infection, SLE systemic lupus erythematosus, HHV human herpes virus



**eTable 7. Performance of Clinical Features in Relation to Disease Risk Score in Patients With Indeterminate Infection Status (Combined Probable Bacterial, Unknown, and Probable Viral Groups)**

	Patients split by DRS score		P value
	DRS predicts viral infection	DRS predicts bacterial infection	
Number of patients	95	80	
Shock (needed inotropes) %	22 of 95 (23%)	35 of 80 (44%)	<b>0.006</b>
Respiratory failure requiring ventilation %	46 of 95 (48%)	51 of 80 (64%)	<b>0.048</b>
Requiring intensive care admission %	51 of 95 (54%)	54 of 80 (68%)	0.066
White blood count (x 10 <sup>3</sup> /mm <sup>3</sup> ): median (IQR) <sup>a</sup>	11.1 (7.3-16.0)	14.1 (8.3-19.4)	0.079
Neutrophil count (x 10 <sup>3</sup> /mm <sup>3</sup> ): median (IQR) <sup>a</sup>	6.8 (3.5-11.4)	8.7 (5.0-13.8)	0.114
CRP during illness (mg/l) <sup>a</sup> (IQR)	71 (27-120)	101 (48-192)	<b>0.015</b>
Respiratory infection: CXR consolidation %	43 of 69 (62%)	47 of 66 (71%)	0.3612
Respiratory infection: no CXR focal change %	24 of 69 (35%)	18 of 66 (27%)	0.3599

<sup>a</sup> with available data. Maximum values in illness used.

DRS – Disease Risk Score; IQR – interquartile range; CRP – C reactive protein; CXR – chest X-ray

Clinical features of children in the three indeterminate groups (Probable Bacterial, Unknown and Probable Viral) were classified. For each clinical feature, the proportion of children with a DRS (the combined *IFI44L* and *FAM89A* expression values) predictive of viral or of bacterial infection was compared using Fisher exact test and two tailed t-tests. Disease Risk Score predictive of bacterial infection was significantly associated with shock, ventilation and higher CRP.

## eReferences

1. Pathan, N., et al., *Role of interleukin 6 in myocardial dysfunction of meningococcal septic shock*. *Lancet, The*, 2004. **363**(9404): p. 203-9.
2. Petty, R.E., et al., *International League of Associations for Rheumatology classification of juvenile idiopathic arthritis: second revision, Edmonton, 2001*. *J Rheumatol*, 2004. **31**(2): p. 390-2.
3. R core development team, *R: a language and environment for statistical computing*. 2011.
4. Schmid, R., et al., *Comparison of normalization methods for Illumina BeadChip HumanHT-12 v3*. *BMC Genomics*, 2010. **11**: p. 349.
5. Jolliffe, I.T., *Principal Component Analysis*. 1986: Springer-Verlag.
6. Friedman, J., T. Hastie, and R. Tibshirani, *Regularization Paths for Generalized Linear Models via Coordinate Descent*. *J Stat Softw*, 2010. **33**(1): p. 1-22.
7. Kaforou, M., et al., *Detection of tuberculosis in HIV-infected and -uninfected African adults using whole blood RNA expression signatures: a case-control study*. *PLoS Med*, 2013. **10**(10): p. e1001538.
8. Robin, X., et al., *pROC: an open-source package for R and S+ to analyze and compare ROC curves*. *BMC Bioinformatics*, 2011. **12**: p. 77.
9. Youden, W.J., *Index for rating diagnostic tests*. *Cancer*, 1950. **3**(1): p. 32-5.
10. Leek, J.T., et al., *The sva package for removing batch effects and other unwanted variation in high-throughput experiments*. *Bioinformatics*, 2012. **28**(6): p. 882-3.
11. Ramilo, O., et al., *Gene expression patterns in blood leukocytes discriminate patients with acute infections*. *Blood*, 2007. **109**(5): p. 2066-77.
12. Hu, X., et al., *Gene expression profiles in febrile children with defined viral and bacterial infection*. *Proc Natl Acad Sci U S A*, 2013. **110**(31): p. 12792-7.
13. Berry, M.P., et al., *An interferon-inducible neutrophil-driven blood transcriptional signature in human tuberculosis*. *Nature*, 2010. **466**(7309): p. 973-7.
14. Suarez, N.M., et al., *Superiority of transcriptional profiling over procalcitonin for distinguishing bacterial from viral lower respiratory tract infections in hospitalized adults*. *J Infect Dis*, 2015. **212**(2): p. 213-22.
15. Benjamini, Y. and Y. Hochberg, *Controlling the False Discovery Rate - a Practical and Powerful Approach to Multiple Testing*. *Journal of the Royal Statistical Society Series B-Methodological*, 1995. **57**(1): p. 289-300.
16. Smyth, G.K., *Linear models and empirical bayes methods for assessing differential expression in microarray experiments*. *Stat Appl Genet Mol Biol*, 2004. **3**: p. Article3.
17. <http://geneontology.org/>.
18. Thomas, P.D., et al., *PANTHER: a library of protein families and subfamilies indexed by function*. *Genome Res*, 2003. **13**(9): p. 2129-41.